

# ELECTRON CYCLOTRON CURRENT DRIVE EXPERIMENTS ON DIII-D \*

R. A. JAMES, G. GIRUZZI,<sup>†</sup> A. FYARETDINOV,<sup>¶</sup> B. DE GENTILE,<sup>†</sup>  
YU. GORELOV,<sup>¶</sup> R. HARVEY,<sup>‡</sup> S. JANZ,<sup>§</sup> J. LOHR,<sup>‡</sup> T. C. LUCE,<sup>‡</sup> K. MATSUDA,<sup>‡</sup>  
P. POLITZER,<sup>‡</sup> R. PRATER,<sup>‡</sup> L. RODRIGUEZ,<sup>†</sup> R. SNIDER,<sup>‡</sup> V. TRUKHIN<sup>¶</sup>

Lawrence Livermore National Laboratory  
University of California  
Livermore, California, USA

UCRL-JC--102929

DE90 010758

Electron Cyclotron Current Drive (ECCD) experiments on the DIII-D tokamak have been performed using 60 GHz waves launched from the high field side of the torus. Preliminary analysis indicates rf driven currents between 50 and 100 kA in discharges with total plasma currents between 200 and 500 kA. These are the first ECCD experiments with strong first pass absorption, localized deposition of the rf power, and  $\tau_E$  much longer than the slowing-down time of the rf generated current carriers. The experimentally measured profiles for  $T_e$ ,  $n_e$  and  $Z_{eff}$  are used as input for a 1D transport code and a multiple-ray, 3D ray tracing code. Comparisons with theory and assessment of the influence of the residual electric field, using a Fokker-Planck code, are in progress. The ECH power levels were between 1 and 1.5 MW with pulse lengths of about 500 msec.

ECCD experiments<sup>1</sup> worldwide are motivated by issues relating to the physics and technical advantages of the use of high frequency rf waves to drive localized currents.<sup>2</sup> ECCD is accomplished by preferentially heating electrons moving in one toroidal direction, reducing their collisionality and thereby producing a non-inductively driven toroidal current.<sup>3</sup>

The poloidal cross section for a typical discharge used in these experiments is shown in Fig. 1. These discharges are limited on the inside wall, with the ECH fundamental resonance ( $B_T = 2.14$  T) located at  $R_{res} = 1.6$  m and the magnetic center located between  $1.55$  m  $< R_m < 1.60$  m. Diagnostics consist of: a) radial electron cyclotron emission (ECE) for  $T_e(r)$ , b) CO<sub>2</sub> interferometry for  $n_e(r)$  and c) visible bremsstrahlung for  $Z_{eff}(r)$ .

<sup>†</sup> Association Euratom-CEA, TORE SUPRA, Cadarache, France.

<sup>¶</sup> Kurchatov Institute, Moscow, USSR.

<sup>‡</sup> General Atomics, San Diego, Ca.

<sup>§</sup> University of Maryland, College Park, Md.

MASTER  
DISTRIBUTION OF THIS DOCUMENT IS UNLIMITED  
90

The launching hardware, located on the inside wall at  $z = +13$  cm, consists of 8 sub-reflectors aimed at  $+15^\circ$  and one aimed at  $+30^\circ$ . These angles are relative to perpendicular injection along the major radius and "+" indicates a direction such as to drive an rf current parallel to  $I_P$ . The experimental antenna pattern is approximately a Gaussian beam with a  $10^\circ$   $1/e$  half-width.

## METHODS OF ANALYSIS

For all discharges, the total toroidal current was held constant by using the constant  $I_P$  feedback circuit. As a result of the ECH, the loop voltage is reduced below its Ohmic value during rf injection by two concurrent processes. The first is a reduction of the global resistance of the plasma, which results as the thermal electron temperature increases, and the second is the presence of rf current drive.

Since a small inductive voltage remains during the rf phase, a two step process is applied in order to calculate  $I_{rf}$ . First the global change in the resistance of the plasma during the rf phase is quantified by measuring changes in  $T_e$  and  $Z_{eff}$ . With  $I_P$  fixed, this procedure is equivalent to determining the inductive voltage necessary to drive all the toroidal current during the rf phase. Differences between this calculation and the measured loop voltage are then attributed to the presence of an rf driven current.

Combining the steady-state circuit equation during the rf phase,  $I_P = [V_i(ezp)/R(rf)] + I_{rf}$ , with that of the Ohmic phase,  $I_P = V_i(oh)/R(oh)$ , we get:

$$I_{rf} = I_P \left[ 1 - \frac{V_i(ezp) R(oh)}{V_i(oh) R(rf)} \right] \quad (1)$$

where  $V_i(ezp)$  is the experimental loop voltage and  $R$  is the plasma resistance. By setting  $I_{rf} = 0$  in Eq. (1), we can determine the inductive voltage that would be necessary during the rf phase to drive all the toroidal current:  $V_i^* = V_i(oh)[R(rf)/R(oh)]$ . Combining this with Eq. (1) gives the desired equation for  $I_{rf}$ :

$$I_{rf} = I_P \left[ \frac{V_i^* - V_i(ezp)}{V_i^*} \right] \quad (2)$$

## EXPERIMENTAL RESULTS

Figure 2 shows the time history for discharge #65218: plasma current ( $I_P$ ), ECH power, loop voltage, central electron temperature, line averaged electron density, magnetic center ( $R_m$ ), and the first time derivative of the sum of currents flowing in the Ohmic and equilibrium field coils. The loop voltage is proportional to the last signal. The discharge has obtained a "stationary state" since all quantities have stopped evolving by  $t = 2200$  ms.

As defined,  $V_1^*$  is the inductive voltage necessary to drive all the plasma current during the rf phase. This is calculated by a 1D transport code<sup>4</sup> using as inputs the experimental measurements of  $I_P$  and the radial profiles for  $T_e(r)$ ,  $n_e(r)$  and  $Z_{\text{eff}}(r)$ . The profile data is used to calculate the plasma's global resistance. Bootstrap current, less than 10% of the total current, is included in the code calculations. The transport code calculates  $V_1^* = 0.7$  V in the Ohmic phase, within 5% of the experimental value, and  $V_1^* = 0.4$  V during rf injection. During the rf phase,  $V_1(\text{exp}) = 0.33$ , thus Eq. (2) gives  $I_{\text{rf}} = 70$  kA.

A 3D, ray tracing code<sup>5</sup> is used to study the ray trajectories and determine the first pass absorbed power. The launched radiation pattern is represented by 30 rays, and the resulting trajectories in the poloidal plane are shown in Fig. 3. Over 99% of the incident power is absorbed and deposited on the inboard side of the resonance. Of the rays that are not fully absorbed, their first pass attenuation averages about 98%.

Using the same experimental profiles and an electric field of 0.03 V/m, a bounce-averaged Fokker-Planck (F.P.) code<sup>6</sup> calculates  $I_{\text{rf}}(\text{F.P.}) = 95$  kA. The influence of the electric field and a comparison with theory are presently being evaluated. The code indicates that damping takes place near  $2v_{\text{th}}$ . The slowing down time, or thermalization time for these energetic electrons ( $\tau_s \simeq 1$  msec) is such that they should completely thermalize before being lost,  $\tau_e \simeq 35$  msec. The F.P. ECH power deposition profile, Fig. 4(b), compares well with that calculated by the ray tracing code, Fig. 3(b).

The Fokker-Planck code's prediction of the horizontal ECE spectrum is compared to the experimental measurement in Fig. 4. Distortion of the electron distribution is confined to the central 1/3rd of the profile, and is characterized by an average perpendicular temperature of about 15 keV. The strong non-thermal ECE emission at large radii is the result of relativistically downshifted 2nd harmonic emission from the centrally localized energetic electrons. The absence of agreement in the range of  $0.6 \leq r/a \leq 0.8$  is consistent with downshifted 3rd harmonic emission from energetic electrons near the edge of the profile. This suggests that radial transport of these electrons from the core is an important aspect of these discharges, a physics issue not accounted for by the F.P. calculations.

## ACKNOWLEDGMENTS

The Electron Cyclotron Current Drive program at General Atomics combines the talents and efforts from several participants: Lawrence Livermore National Laboratory (LLNL); the University of Maryland; member of the TORE SUPRA group from Cadarache, France (Association Euratom-CEA); and members from the Kurchatov Institute in Moscow, USSR. This work was performed under the auspices of the U.S. Department of Energy by Lawrence

## REFERENCES

1. Lloyd, B., *et al.*, Nucl. Fusion **28**, 1013 (1988) and H. Tanaka, *et al.*, Phys. Rev. Lett. **60**, 1033 (1988).
2. Prater, R., Eighth Topical Conference on Radio-Frequency Power in Plasmas, AIP Conference Proceedings No. 190 (AIP, New York, 1989), p. 22.
3. Fisch, N.J., Rev. Mod. Phys. **59**, 175 (1987).
4. Pfeiffer, W.W., *et al.*, General Atomics report GA-A16178 (1980).
5. Matsuda, K., IEEE Transactions on Plasma Science **17**, 6 (1989).
6. Giruzzi, G., Phys. Fluids **31**, 3305 (1988).

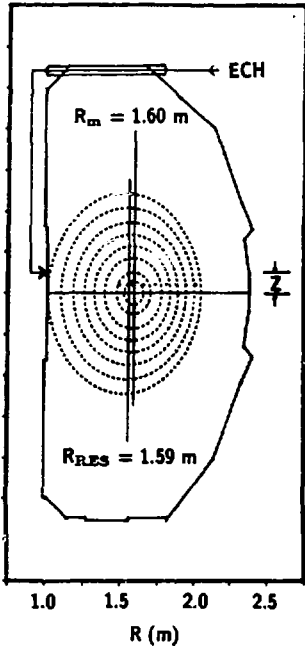


Fig. 1. Poloidal cross section for discharge #65218 at 2370 msec.

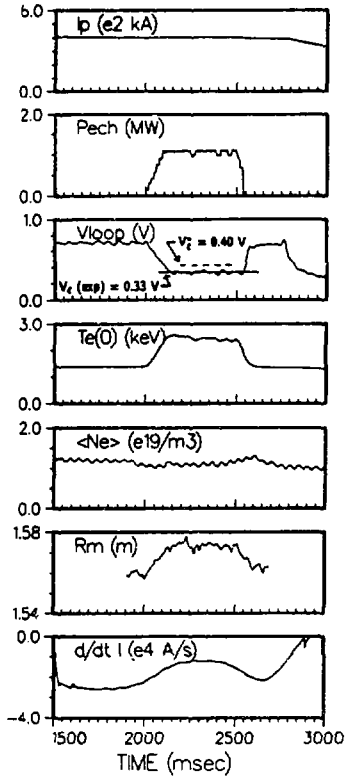


Fig. 2. Time evolution for discharge #65218.

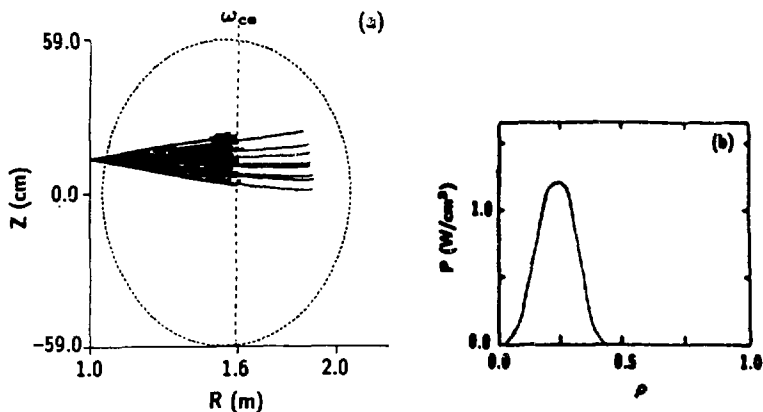


Fig. 3. (a) Ray trajectories, and (b) ECH deposition profile from ray tracing code for discharge #65218 at 2370 msec.

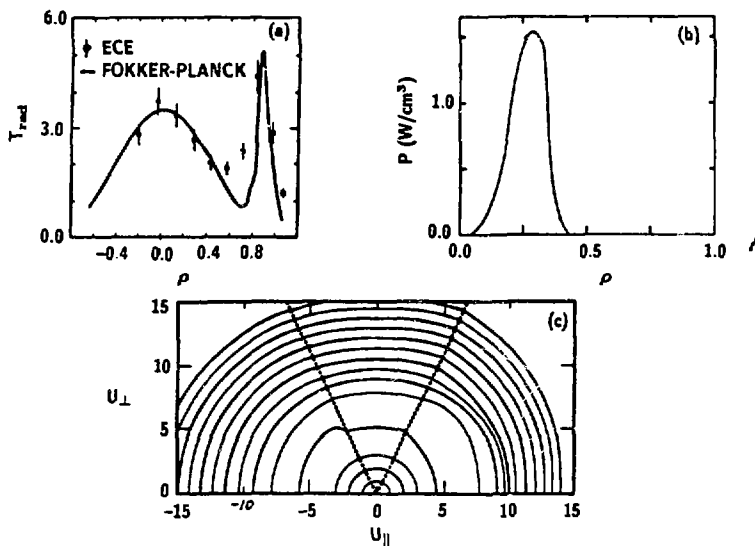


Fig. 4. (a)  $T_{rad}(\rho)$  from ECE and Fokker-Planck code, (b) ECH deposition profile from Fokker-Planck code, and (c) computed distribution function at  $\rho = 0.32$ , momenta normalized to  $(m_e T_e)^{1/2}$ .

#### DISCLAIMER

This document was prepared as an account of work sponsored by an agency of the United States Government. Neither the United States Government nor the University of California nor any of their employees, makes any warranty, express or implied, or assumes any legal liability or responsibility for the accuracy, completeness, or usefulness of any information, apparatus, product, or process disclosed, or represents that its use would not infringe privately owned rights. Reference herein to any specific commercial products, process, or service by trade name, trademark, manufacturer, or otherwise, does not necessarily constitute or imply its endorsement, recommendation, or favoring by the United States Government or the University of California. The views and opinions of authors expressed herein do not necessarily state or reflect those of the United States Government or the University of California, and shall not be used for advertising or product endorsement purposes.

\* Livermore National Laboratory under Contract No. W-7405-Eng-48 and by General Atomics under Contract No. DE-AC03-89ER51114.